APPLIED PHYSICS LETTERS **88**, 241912 (2006)

Determination of transformation stresses of shape memory alloy thin films: A method based on spherical indentation

Wenyi Yan[a)]
School of Engineering and Information Technology, Deakin University, Geelong, Victoria 3217, Australia

Qingping Sun, Xi-Qiao Feng, and Linmao Qian
Department of Mechanical Engineering, The Hong Kong University of Science and Technology, Clear Water Bay, Kowloon, Hong Kong, China

(Received 10 February 2006; accepted 27 April 2006; published online 14 June 2006)

The forward and reverse transformation processes of superelastic shape memory alloys (SMAs) under spherical indentation are analyzed. We found that there exist two characteristic points, the bifurcating point and the returning point, in an indentation curve. The corresponding bifurcation force and return force, respectively, rely on the forward transformation stress and the reverse transformation stress. A method to determine the transformation stresses of SMA from the measure of the bifurcation and return forces is proposed. Additionally, we suggest a slope approach to determine the values of the two forces with high accuracy. © *2006 American Institute of Physics*. [DOI: 10.1063/1.2213018]

Shape memory alloys (SMAs), such as NiTi, are well known for their extraordinary shape memory and superelastic properties. These properties are due to the intrinsic thermoelastic martensitic transformation under mechanical loading at different temperatures. For instance, in the case of superelasticity, the transformed martensite produced due to mechanical loading can transform back to austenite during unloading, recovering a large amount of the prior deformation. Both the shape memory and the superelastic properties have been exploited to design SMA-based structures. Recently, thin film SMA has been recognized as a promising and high performance material in the field of microelectromechanical system. The reversible phase transformation in shape memory alloys also signals extraordinary mechanical properties such as high wear resistance and interesting dynamic response during indentation.[1–5] In characterizing the mechanical properties of structures in very small dimensions such as thin films, the transformation stresses are usually much more difficult to measure than the traditional bulk samples. This stimulated the present research to perform the spherical indentation of SMAs. We choose a spherical indenter to avoid plastic deformation as in sharp indenters so that we can focus on the contributions of transformation properties on the indentation response.

Consider a typical superelastic NiTi SMA whose simplified stress-strain curve under uniaxial loading is shown in Fig. 1. The forward and reverse transformation processes are treated as perfect, i.e., the forward and reverse transformation stresses σ_f and σ_r, are kept constant during the forward and reverse transformations, respectively. In this simple model, only seven material parameters are used to define the superelastic behavior of a shape memory alloy. Besides σ_f and σ_r, we also have $\varepsilon^{\mathrm{tr}}$, the maximum transformation strain in uniaxial tension, i.e., the maximum magnitude of the transformation strain, E_a and E_m, the elastic Young's modulus of austenite and martensite, and υ_a and υ_m, the Poisson's ratio of austenite and martensite. This model can be easily extended to the case of transformation hardening by adding two more parameters. It must be mentioned that here, E_a and E_m are considered as constant properties, which is a good approximation for many superelastic NiTi alloys at a given temperature.[6,7] Due to the mixture of elastic deformation and a small amount of transformation or martensite reorientation, the apparent E_a and E_m might vary during an apparent elastic loading in some cases,[7,8] which are excluded from the current study.

The bifurcating point and the bifurcation force. We now consider that a rigid diamond spherical indenter tip with radius R is pressed into a superelastic SMA. The finite element method is applied to simulate such a frictionless indentation process by using ABAQUS (Ref. 9) combined with a three dimensional (3D) SMA model.[10] Generally, the indentation force F depends on the indentation depth h and the indenter radius R, as well as the material parameters σ_f, σ_r, E_a, E_m, $\varepsilon^{\mathrm{tr}}$, υ_a, and υ_m, i.e.,

$$F = Z(\sigma_f,\sigma_r,E_a,E_m,\upsilon_a,\upsilon_m,\varepsilon^{\mathrm{tr}},h,R). \quad (1)$$

Before the start of the forward transformation, the material is in a linear elastic state. Within the limits of small deformation, the Hertz contact theory can be applied to describe this purely elastic contact problem. The elastic indentation force before phase transformation is therefore determined by[11]

$$F = \frac{4}{3}E_a^{*}R^{1/2}h^{3/2}, \quad (2)$$

where $E_a^{*}=E_a/(1-\upsilon_a^2)$. Once the maximum equivalent stress inside the material reaches the forward transformation stress,

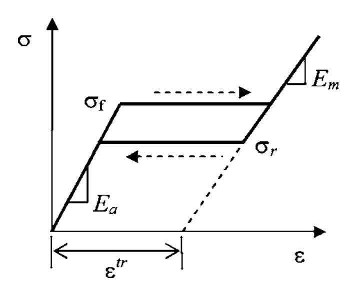

FIG. 1. An idealized superelastic model under uniaxial loading.

[a)]Author to whom correspondence should be addressed; electronic mail: wenyi.yan@deakin.edu.au

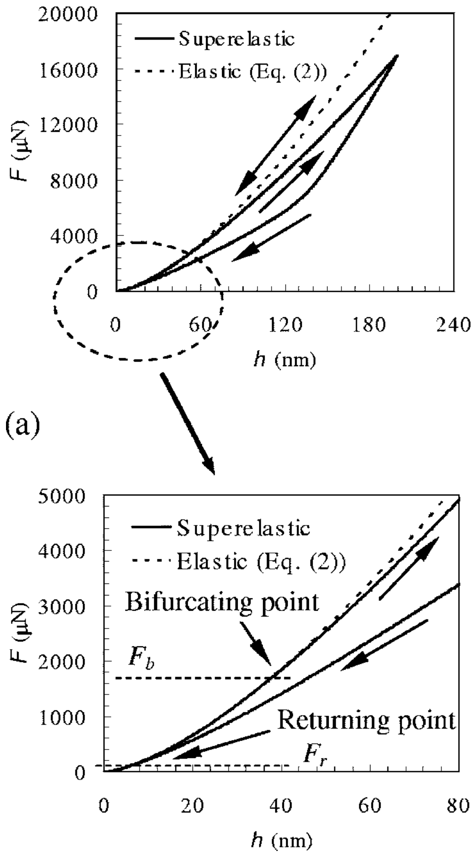

FIG. 2. (a) Comparison between an elastic indentation curve and a superelastic indentation curve, and (b) definitions of the bifurcating point and the corresponding bifurcation force F_b and the returning point and the corresponding return force F_r.

austenite will start to transform to martensite,[10] and the indentation force-depth curve will start to deviate from the pure elastic curve as demonstrated in Fig. 2(a). A bifurcating point can be defined as the point in the indentation loading curve that starts to deviate from the elastic indentation curve, see Fig. 2(b). The force corresponding to the bifurcating point is called the bifurcation force F_b.

Because this bifurcating point signals the start of the forward transformation in the sample, it is an important characteristic point in a superelastic indentation curve. The bifurcation force F_b should not rely on the properties of the product phase, i.e., the elastic Young's modulus and Poisson's ratio of martenite. Furthermore, it does not depend on the degree of hardening of the forward transformation stress-strain curve nor the maximum magnitude of the transformation strain ε^{tr}. In this sense, F_b is analogous to the initial transformation stress σ_f in Fig. 1. However, the bifurcation force is the response of the indented structure and must rely on the properties of the austenite and the geometry of the indenter. Therefore, we have the following functional relationship:

$$F_b = Y(\sigma_f, E_a, \upsilon_a, R). \tag{3}$$

The corresponding dimensionless function is

$$\frac{F_b}{R^2 E_a} = \Pi_1\left(\frac{\sigma_f}{E_a}, \upsilon_a\right). \tag{4}$$

The dimensionless function Eq. (4) can be determined either numerically or analytically by applying Hertz contact theory for small deformation, the latter gives[11]

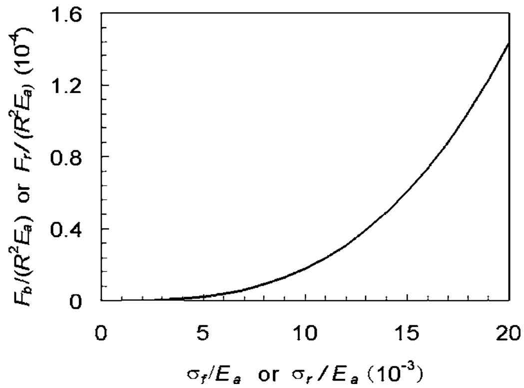

FIG. 3. Relationships between the normalized bifurcation force $F_b/(R^2E_a)$ and the normalized forward transformation stress σ_f/E_a and between the normalized return force $F_r/(R^2E_a)$ and the normalized reverse transformation stress σ_r/E_a for υ_a=0.3 under small deformation condition.

$$\frac{F_b}{R^2 E_a} = 17.92\left(\frac{\sigma_f}{E_a}\right)^3 \tag{5}$$

for υ_a=0.3 as shown in Fig. 3. It is seen that a higher forward transformation stress will result in a higher bifurcation force or vice versa.

The returning point and the return force. During the unloading process, the martensite phase will become unstable and will transform back to the austenite phase for superelastic SMAs. The reverse transformation stress σ_r will now affect the unloading response of the indentation. The dimensionless function for the indentation force during unloading can be expressed as[12]

$$\frac{F}{R^2 E_a} = \Pi_2\left(\frac{\sigma_f}{E_a}, \frac{\sigma_r}{E_a}, \frac{E_m}{E_a}, \varepsilon^{tr}, \upsilon_a, \upsilon_m, \frac{h_m}{R}, \frac{h}{R}\right), \tag{6}$$

where h_m is the maximum indentation depth before unloading. Before the load reduces to zero, the reverse transformation process will be completed for a superelastic SMA. Correspondingly, the final part of the unloading curve will eventually return to the elastic loading-unloading curve as shown in Fig. 2. The returning point indicates the completion of the reverse transformation in the material. The corresponding force at this point is named as the return force F_r. It is another important quantity in a superelastic indentation curve. According to the uniqueness theorem of the solution for an elastic stable problem, we can prove that the return force F_r does not depend on σ_f, E_m, υ_a, ε^{tr}, and the transformation processes.[12] In other words, the return force does not depend on the transformation history, and we have

$$\frac{F_r}{R^2 E_a} = \Pi_3\left(\frac{\sigma_r}{E_a}, \upsilon_a\right). \tag{7}$$

Because the return force corresponds to an elastic field (just at the end of the reverse transformation process) with the maximum equivalent stress equal to σ_r, we have further proved that the dimensionless function Π_1 in (4) for the bifurcation force is identical to the dimensionless function Π_3 in (7) to determine the return force.[12] Within the limits of small deformation, we similarly have the following explicit form for F_r:

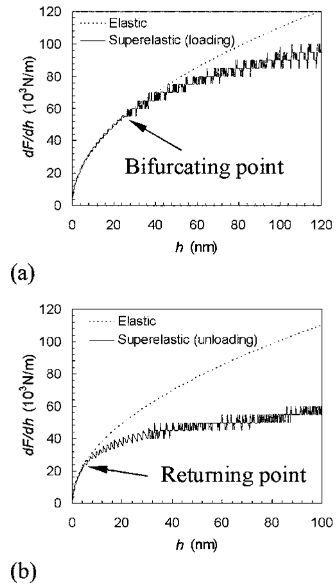

FIG. 4. (a) Determination of the bifurcating point from the elastic slope and superelastic slope curves for the loading process, and (b) determination of the returning point from the elastic slope and superelastic slope curves for the unloading process.

$$\frac{F_r}{R^2 E_a} = 17.92\left(\frac{\sigma_r}{E_a}\right)^3 \tag{8}$$

for $\upsilon_a=0.3$ as shown in Fig. 3. It is seen that if F_b and F_r can be determined from experiment, then σ_f and σ_r can be immediately obtained.

The slope method to determine the bifurcation force and the return force. We can use the relationships (5) and (8) to develop a method to determine the transformation stresses from the measured bifurcation and return forces by a spherical indentation test once we know the elastic constants of the austenite. Obviously, the accuracy of such extracted transformation stresses relies on the accuracy of the measured bifurcation and return forces. Practically, it would be very difficult to obtain their accurate values from the indentation loading and unloading curves. For instance, in the case shown in Fig. 2(b) with $\sigma_f=1000$ MPa, $E_a=50$ GPa, $\upsilon_a=0.3$, and $R=10$ μm, the estimated bifurcation point from the indentation curve is at $h=39$ nm and $F_b=1800$ μN, which is very different from the theoretical point ($h=39$ nm, $F_b=717\mu$N) by Eqs. (2) and (5).

To solve this problem, we propose using the elastic slope and superelastic indentation slope curves in loading and unloading to determine the bifurcating and returning points. The calculated slope curves corresponding to the F-h curves in Fig. 2 are shown in Figs. 4(a) and 4(b), respectively. We can see that the bifurcating and returning points are very distinct and therefore can be more accurately determined. In this example, the theoretical values of F_b and F_r are, respectively, 717 and 46 μN from (5) and (8) for the given SMA sample with $E_a=50$ GPa, $\upsilon_a=0.3$, $\sigma_f=1000$ MPa, $\sigma_r=400$ MPa, and indenter radius $R=10$ μm. From the slope curves in Fig. 4, the bifurcation force and the return force are estimated as 971 and 58.6 μN, which are close to the theoretical values of 717 and 46 μN. The estimated forward and reverse transformation stresses from (5) and (8) or Fig. 3 are, respectively, 1106 and 434 MPa, which are even closer to the theoretical values of 1000 and 400 MPa with about a 10% error since $F\propto(\sigma)^3$. Therefore, we conclude that the proposed slope method is more accurate and reliable to determine the bifurcating point and the returning point, and could be used to extract the transformation stresses from a spherical indentation test. In a real experiment, the extracting procedure is as follows:

(a) Draw the superelastic indentation loading slope and unloading slope curves from the measured spherical indentation loading and unloading curves.
(b) Draw the elastic indentation slope curve based on Hertz elastic contact theory in the same diagram as shown in Fig. 4 for comparison.
(c) Determine the bifurcating point by comparing the elastic indentation slope curve with the superelastic loading slope curve. The indentation depth h_b corresponding to the bifurcating point can be extracted and the bifurcation force F_b can be determined from Eq. (2).
(d) Determine the forward transformation stress σ_f according to Eq. (5) or Fig. 3.
(e) Determine the returning point by comparing the elastic slope and superelastic unloading slope curves. The indentation depth and force (h_r, F_r) corresponding to the returning point can be obtained as in (c).
(f) Determine the reverse transformation stress σ_r according to Eq. (8) or Fig. 3.

In summary, we have identified two characteristic points, the bifurcating and returning points, by comparing the pure elastic indentation curve with the superelastic indentation curve. We proved that the corresponding bifurcation and return forces uniquely rely on the forward and reverse transformation stresses of the material, respectively, besides the elastic constants of the austenite and the indenter tip radius R. These unique relationships provide the theoretical basis for the proposed method to determine the transformation stresses of small samples such as thin films from the measured values of the two forces. In order to improve the accuracy of the results, an indentation slope method is further proposed to locate the bifurcating and returning points and therefore to determine the two forces. The proposed method would be very convenient to implement in a real experiment and also have the potential to characterize the transformation properties of other material systems at a very small scale by using the micro-/nanoindentation technique.

This study was supported by the Research Grants Council of the Hong Kong Special Administrative Region, China, through Project Nos. HKUST 6199/03E and 619705.

[1]L. Qian, X. Xiao, Q. Sun, and T. Yu, Appl. Phys. Lett. **84**, 1076 (2004).
[2]D. Y. Li, Smart Mater. Struct. **9**, 717 (2000).
[3]K. Gall, K. Juntunen, H. J. Maier, H. Sehitoglu, and Y. I. Chumlyakov, Acta Mater. **49**, 3205 (2001).
[4]W. Ni, Y.-T. Cheng, and D. S. Grummon, Appl. Phys. Lett. **82**, 2811 (2003).
[5]X.-G. Ma and K. Komvopoulos, Appl. Phys. Lett. **84**, 4274 (2004).
[6]J. A. Shaw and S. Kyriakides, J. Mech. Phys. Solids **43**, 1243 (1995).
[7]Y. Liu and H. Xiang, J. Alloys Compd. **270**, 154 (1998).
[8]C. P. Frick, A. M. Ortega, J. Tyber, K. Gall, and H. J. Maier, Metall. Mater. Trans. A **35A**, 2013 (2004).
[9]Hibbitt, Karlsson and Sorensen Inc., ABAQUS, version 6.4, Providence, RI, 2004.
[10]F. Auricchio and R. L. Taylor, Comput. Methods Appl. Mech. Eng. **143**, 175 (1997).
[11]K. L. Johnson, *Contact Mechanics* (Cambridge University Press, London, 1985).
[12]W. Yan, Q. Sun, X. Feng, and Q Lian, Int. J. Solids Struct. (in press).